Đánh giá tiềm năng của than sinh học biến tính từ lõi ngô trong việc loại bỏ thuốc nhuộm Crystal Violet

TÓM TẮT

Sự tồn tại của các thuốc nhuộm tổng hợp trong nước thải gây ra những ảnh hưởng nghiêm trọng đến môi trường và sức khỏe con người do cấu trúc phức tạp, khó phân hủy sinh học, tích lũy sinh học và độc tính cao. Trong đó, Crystal Violet (CV) là thuốc nhuộm thuộc nhóm triphenylmethane có độc tính mạnh, có khả năng gây đột biến và ung thư ở động vật có vú. Nghiên cứu này nhằm đánh giá khả năng loại bỏ CV trong nước bằng vật liệu than sinh học chế tạo từ lõi ngô. Các mẫu than sau biến tính hóa học thể hiện đặc tính nổi bật như diện tích bề mặt riêng cao (989.14 m^2/g), thể tích lỗ xốp lớn (1.5 cm^3/g) và sự hiện diện của các nhóm chức hoạt động trên bề mặt. Kết quả cho thấy mẫu BioP-Na 400 đạt hiệu quả cao nhất, với hiệu suất loại bỏ 97.2% và dung lượng hấp phụ cực đại 116.68 mg/g ở nồng độ CV ban đầu 30 mg/L trong 60 phút. Dữ liệu hấp phụ phù hợp với mô hình đẳng nhiệt Langmuir ($R^2 = 0.982$), cho thấy quá trình xảy ra chủ yếu theo cơ chế hấp phụ đơn lớp trên bề mặt đồng nhất. Động học tuân theo mô hình giả bậc hai (PSO), chứng tỏ hấp phụ vật lý chiếm ưu thế, có sự hỗ trợ của tương tác hóa học nhẹ. Kết quả nghiên cứu khẳng định than sinh học biến tính từ lõi ngô là vật liệu hấp phụ hiệu quả, thân thiện môi trường và chi phí thấp, có tiềm năng ứng dụng trong xử lý nước thải chứa thuốc nhuộm, góp phần thúc đẩy các giải pháp bền vững trong bảo vệ môi trường.

Keywords: Hấp phụ, lõi bắp, crystal violet, xử lý thuốc nhuộm, than sinh học biến tính

Assessing the potential of modified biochar derived from corn cob for the elimination of Crystal Violet dye

ABSTRACT

The presence of synthetic dyes in wastewater poses serious environmental and health risks due to their complex aromatic structures, non-biodegradability, bioaccumulation, and toxicity. Among them, crystal violet (CV) is a highly toxic triphenylmethane dye, known for its mutagenic and carcinogenic effects on mammals. This study aimed to evaluate the removal performance of CV in aqueous solutions using corn cob-based biochar. The chemically modified biochars exhibited excellent characteristics, including a high specific surface area (up to 989.14 m^2/g), large pore volume (1.5 cm^3/g), and an abundance of functional groups on their surfaces. The experimental results revealed that BioP-Na 400 exhibited the highest performance, achieving 97.2% removal efficiency and a maximum adsorption capacity of 116.68 mg/g at a CV concentration of 30 mg/L within 60 minutes. Adsorption equilibrium was best described by the Langmuir isotherm model (R^2 = 0.982), and kinetics followed a pseudo-second-order model, indicating that the chemisorption was included in the adsorption process while physical adsorption dominated. These findings can provide significant insights into mitigating environmental pollution using materials derived from agricultural waste, which are low-cost, eco-friendly, and effective in removing dyes from wastewater.

Keywords: Adsorption, corn cob, crystal violet, dye removal, modified biochar

1. INTRODUCTION

Rapid industrialization and urbanization have significantly intensified environmental concerns, particularly water pollution caused by the release of industrial effluents. Wastewater from those sectors, including textiles, paper, leather tanning, food, cosmetics, and pharmaceuticals, typically contains synthetic dyes, which are recognized as one of the most persistent sources of pollution due to their complex aromatic structures, stability, and resistance to biodegradation.[1] These pollutants that endure in the environment for long periods exert harmful effects on aquatic ecosystems and human health. It has been estimated that over 600,000 tons of dye-containing wastewater are discharged into the environment annually.[1]

Among synthetic dyes, triphenylmethane dyes are particularly hazardous due to their widespread industrial applications and potential toxicity. Crystal violet (CV), chemically known as hexamethyl pararosaniline chloride ($C_{25}H_{30}N_3Cl$), is a typical cationic dye of this group. It appears purple-blue in aqueous solution (λ_{max} = 590 nm, pKa = 9.34) and is widely used in textile dyeing, printing inks, paints, biological staining (e.g., Gram staining of bacteria), and veterinary medicine as an antifungal and antiparasitic agent.[2-4] However, wastewater containing CV poses serious environmental and health concerns. CV has been reported to act as a mitotic poison, clastogen, and tumor promoter, and both CV and its leuco form have shown carcinogenicity and mutagenicity in mammals, causing damage to the liver, kidney, and lungs.[5, 6] Moreover, CV contamination inhibits photosynthesis in aquatic plants, disrupts seed germination, and persists in sediments, where it can accumulate in aquatic organisms.[5, 6]

Numerous treatment techniques have been investigated to reduce the impact of CV on the environment, including ion-exchange membranes, coagulation–flocculation, photocatalysis, ozonation, electrochemical oxidation, and advanced oxidation processes such as Fenton (Fe^{2+}/H_2O_2), as well as biological degradation. Despite their effectiveness, these processes often involve high operational costs, energy consumption, or the generation of secondary pollutants. In contrast, adsorption has emerged as one of the most promising approaches due to its cost-effectiveness, simplicity, environmental compatibility, and high efficiency even at low dye concentrations.[7] Various adsorbents, such as activated carbon, composites, zeolitic imidazolate frameworks (ZIFs), and graphene-based materials, have been explored. Recently, biochar derived from agricultural residues has attracted increasing attention due to its large surface area, porous structure, abundant functional groups, and cation exchange capacity, which together favor the adsorption of persistent organic pollutants.[8, 9]

Biochar is generally produced through pyrolysis of lignocellulosic biomass under oxygen-limited conditions. While pristine biochar exhibits promising structural properties, its limited surface functional groups often reduce its adsorption efficiency for organic pollutants. Therefore, physical and chemical modifications, such as activation with acids or bases, have been widely employed to enhance its performance.[8, 9] Modified biochar has demonstrated improved porosity, surface

area, and functional groups, thereby facilitating efficient adsorption of contaminants, including pesticides, antibiotics, heavy metals, and dyes.[8, 10]

Vietnam, as an agricultural country, produces a substantial amount of farming residues annually. Corncob, a byproduct of maize cultivation, contains cellulose, hemicellulose, lignin, and proteins, making it a potential precursor for biochar production.[11] Although corncobs are sometimes used as fuel or for mushroom cultivation, a large portion is discarded, contributing to environmental pollution. Transforming corncobs into modified biochar for wastewater treatment not only offers a sustainable solution for waste management but also provides an inexpensive and effective material for dye adsorption. However, corn cob-based materials for CV removal from aqueous solution have been rarely investigated, hindering a comprehensive understanding of the fundamentals of removal performance and mechanisms of CV adsorption. This may cause limited further applications.

The present study aims to evaluate the performance of corn cob-based biochars for removing crystal violet from aqueous solutions. Various characterization techniques, including SEM, FTIR, EDX, and BET, were employed to examine the physicochemical properties of the biochar and its adsorption mechanisms. Kinetic and isotherm adsorption models were applied to determine the adsorption behavior of CV on biochar surfaces. This work offers scientific insights into the valorization of agricultural residues as efficient adsorbents, contributing to sustainable approaches for wastewater treatment.

2. MATERIALS AND METHOD

2.1. Materials

Corn cobs were collected from local agricultural waste in Cai Rang Ward, Can Tho City. Crystal violet (CV, $C_{25}H_{30}ClN_3$, ≥ 99% purity), NaOH, and H_3PO_4 were purchased from Xilong Chemical Co., Ltd. (China). All solutions were prepared using deionized water

2.2. Preparation and characterization of biochar

The dried corn cobs were cut into pieces of 2–5 mm and subjected to pyrolysis in a muffle furnace under limited oxygen conditions at three temperatures: 400, 500 and 600 °C for 2 hours, with a heating rate of 10 °C/min. The obtained biochars were denoted as Bio-400, Bio-500, and Bio-600.[12]

For chemical modification, two activation agents were used. In the NaOH activation, biochar samples were impregnated with 1M NaOH solution at a solid-to-liquid ratio of 1:10 (g/mL) for 12 hours, followed by drying and calcination at the corresponding pyrolysis temperature. The samples were then thoroughly washed with deionized water until neutral pH and dried at 105°C. Similarly, H_3PO_4 modification was performed with 1M H_3PO_4 solution. The resulting materials were named BioP-Na 400/500/600, depending on the chemical treatment and pyrolysis temperature.[12]

2.3. Adsorption experiments

Batch adsorption experiments were performed to evaluate the CV removal efficiency. In a typical experiment, 20 mL of

dye solution was mixed with a defined amount of biochar and agitated at 400 rpm. After adsorption, the mixtures were centrifuged at 4000 rpm for 10 min, and the residual dye concentration was analyzed by UV-Vis spectrophotometry at 590 nm.

The removal rate (R) and the adsorption capacity (Q_t) at time t were calculated according to Equations (1) and (2) as follows.

$$R(\%) = \frac{C_0 - C_t}{C_0} \times 100 \quad (1)$$

$$Q_t\left(\frac{mg}{g}\right) = \frac{(C_0 - C_t) \times V}{w} \quad (2)$$

where C_0 (mg/L) and C_t (mg/L) are the initial and residual CV concentrations at time t (mg/L), V(L) represents the solution volume, and w (g) is the mass of adsorbent used.

2.4. Adsorption experiments

A kinetic study determines the effect of contact time on the adsorption capacity of the adsorbents and provides insights into the possible adsorption mechanisms occurring during the process.[13] Understanding the adsorption mechanism is essential for predicting solid–liquid interactions and designing efficient treatment systems. In this study, the kinetic adsorption experiments were carried out with a CV concentration of 30 mg/L, an adsorbent dosage of 0.25 g/L, and a contact time ranging from 5 to 150 min at room temperature. The mixtures were agitated at 400 rpm, then separated by centrifugation, and the residual CV concentration was determined using a UV–Vis spectrophotometer at 590 nm. The kinetic pseudo-first-order (PFO, equation 3), pseudo-second-order (PSO, equation 4), and Elovich (equation 5) models were applied to describe the adsorption process.[13-15]

Pseudo-first-order model (PFO):

$$q_t = q_e \times \left[1 - \exp\left(-\frac{k_1 t}{2.303}\right)\right] \quad (3)$$

Pseudo-second-order model (PSO):

$$\frac{t}{q_t} = \frac{1}{k_2 q_e^2} + \frac{t}{q_e} \quad (4)$$

The initial adsorption rate h can be determined from the PSO kinetic parameters as follows.

$$h = k_2 Q_e^2$$

Elovich model

$$q_t = \frac{1}{\beta}\ln(\alpha\beta) + \frac{1}{\beta}\ln(t) \quad (5)$$

where q_t (mg/g) is the adsorption capacity at time; t (min), qe (mg/g) is the equilibrium adsorption capacity, k_1 (min^{-1}) and k_2 ($g^{-1}.min^{-1}$) are the rate constants of the PFO and PSO models, respectively, h is the initial adsorption rate (mg/(g.min), α (mg/(g.min)) and β (g/mg) are constants of the Elovich model. For porous biochar, a larger C value indicates a greater boundary layer effect, while a lower C value reflects higher surface heterogeneity and availability of active sites.[14, 16]

Adsorption isotherm experiments were carried out to investigate the equilibrium interaction between CV and biochar, providing important information about adsorption capacity and adsorption behavior. The isotherm studies were conducted with initial CV concentrations ranging from 10 to 120 mg/L, an adsorbent dosage of 0.25 g/mL, and an agitation speed of 400 rpm until equilibrium was

reached. The experimental data were fitted to the Langmuir (equation 7), Freundlich (equation 9), and Dubinin–Radushkevich (D–R, equation 10) models.[14, 15]

Langmuir models.

$$q_e = \frac{K_L.Q_m.C_e}{1+K_L.C_e} \quad (7)$$

Where q_m is the theoretical maximum adsorption capacity (mg/g), and K_L denotes the Langmuir equilibrium constant related to the surface heterogeneity; therefore, it refers to the adsorption strength. A separation factor (or equilibrium parameter), R_L, a dimensionless constant that describes the characteristics of the Langmuir isotherm, is defined as follows.

$$R_L = \frac{1}{1+K_L.C_o} \quad (8)$$

The value of R_L shows the type of the isotherm: unfavorable ($R_L > 1$), linear ($R_L = 1$), favorable ($0 < R_L < 1$), or irreversible (($R_L = 0$).[15, 16]

Freundlich model.

$$q_e = K_F.C_e^{1/n} \quad (9)$$

where K_F (mg.g/(L.mg^{-1})$^{1/n}$) and n represent the Freundlich rate constant referring to adsorption capacity and adsorption intensity, respectively.

Dubinin-Radushkevich model (D-R model).

$$q_e = q_0.\exp(-K_{DR}\varepsilon^2) \quad (10)$$

$$\varepsilon = RT\left(1+\frac{1}{C_e}\right)$$

$$E = \frac{1}{\sqrt{2K_{DR}}}$$

where K_{DR} (mol^2/kJ^2) is the D-R rate constant related to adsorption energy, E (kJ/mol) is the average adsorption energy per molecule of adsorbate required to transfer one mole of the adsorbate from the solution to the adsorbent surface, ε denotes the Polanyi adsorption potential which is a function of temperature, R is the ideal gas constant, 8.314 J/(mol.K), and T is the absolute temperature (K).

The non-linear mathematical models were fitted and plotted in OriginPro 2022 v.9.9.0225 (SR1) software.

3. RESULTS AND DISCUSSION

3.1. Biochar characterization

The physicochemical properties of raw corncob and biochar samples prepared at different pyrolysis temperatures with and without NaOH and H_3PO_4 activation were thoroughly characterized to elucidate their influence on crystal violet (CV) adsorption. Elemental composition analysis Error! Reference source not found. showed that the pristine corncob contained 48.48 wt.% C and 42.02 wt.% O, indicating the dominance of cellulose, hemicellulose, and lignin in the biomass structure. After pyrolysis at 400 °C, the carbon content increased to 71.54 wt.% while oxygen decreased to 24.94 wt.%, reflecting partial decomposition of oxygenated functional groups. Activation with NaOH and H_3PO_4 at the same temperature further improved carbonization, with BioP-Na 400 containing 77.87 wt.% C and 20.63 wt.% O. This enrichment of carbon alongside the reduction of oxygen suggested an increase in aromaticity

and graphitization of the biochar, which is favorable for π–π interactions with the aromatic rings of CV. At higher pyrolysis temperatures (500–600°C), the carbon content continued to rise, reaching 88.86 wt.% for BioP-Na 600, while oxygen was significantly depleted (8.86 wt.%). This behavior indicates extensive devolatilization and condensation of carbon skeletons, consistent with previous reports on biomass pyrolysis. However, excessive carbonization may reduce the number of oxygen-containing groups essential for electrostatic attraction and hydrogen bonding with cationic dyes

Table 1. *Basic physicochemical characteristics of various materials.*[12]

Sample	C (wt.%)	O (wt.%)	P (wt.%)	Na (wt.%)	S_{BET} (m^2/g)	S_{BJH} (m^2/g)	Pore volume (cm^3/g)	Pore size (nm)
Corncob	48.48	42.02	0.37	-	-	-	-	-
Bio 400	71.54	24.94	0.14	-	1.28	-	0.0037	0.78
BioP-Na 400	77.87	20.63	0.47	1.03	989.14	909.79	0.61	2.71
BioP-Na 500	76.73	21.41	0.34	1.53	-	774.28	0.34	0.96
BioP-Na 600	88.86	8.86	1.69	0.58	-	2003.78	1.5	0.98

The thermogravimetric analysis (TGA) curve of corncob is presented in **Figure 1a**. The thermal degradation of the sample occurred in three distinct stages. The initial mass loss of about 9.36% was observed below 150 °C, which can be attributed to the evaporation of physically adsorbed water and the release of light volatiles. In the second stage (180–350°C), the mass sharply decreases by 51.91%, mainly due to the decomposition of hemicellulose and a portion of cellulose. Finally, during the third stage (350–1000°C), a further weight loss of 38.49% occurs, attributed to the degradation of lignin along with the remaining cellulose from the previous stage. This decomposition is slower and less distinct compared to stages 1 and 2, indicating that lignin requires higher temperatures and longer reaction times for complete thermal degradation. Under the influence of high temperatures during pyrolysis, the side chains of cellulose and hemicellulose are broken down into smaller organic molecules, which volatilize, leading to a reduction in sample mass. Consequently, volatile organic compounds are released, leaving behind a carbon-rich residue.

The surface area and porosity analyses clearly showed the effect of chemical activation compared with simple pyrolysis. Bio 400 exhibited a very low surface area of only 1.28 m^2/g, indicating poor porosity development. In contrast, the modified samples displayed significantly improved textural properties. BioP-Na 400 achieved the highest S_{BET} is 989.14 m^2/g with a S_{BJH} value of 909.79 m^2/g, while BioP-Na 500 and BioP-Na 600 also exhibited substantial surface areas (774.28 and 2003.78 m^2/g, respectively). These values indicate the successful development of a well-defined mesoporous structure, which can provide abundant adsorption sites and facilitate intraparticle diffusion of CV molecules.

FTIR analysis in **Figure 1b** confirmed the presence of characteristic functional groups in Bio 400 as well as in the modified BioP-Na samples prepared at different pyrolysis temperatures. A broad and intense absorption band around 3300 cm^{-1} indicated the presence of hydroxyl (–OH) groups, while the peaks near 2900 cm^{-1} corresponded to the stretching vibrations of C–H bonds. Variations in the intensity and position of the peaks in the region of 1700–1500 cm^{-1}, particularly those associated with alkenyl (C=C) groups, suggested differences in the structural or chemical composition among the samples. In addition, absorption bands observed near 1200 cm^{-1}, attributed to C–O stretching vibrations, also highlighted structural diversity. Shifts in both the position and intensity of these peaks demonstrated that chemical activation with NaOH and H_3PO_4 significantly affected the environment of surface functional groups, thereby altering the overall structure of the biochar.

Surface morphology analysis by SEM **Figure 1c** further confirmed the structural characteristics of BioP-Na 400. The biochar exhibited a rough surface with a highly porous and irregular honeycomb-like architecture, typical of a carbonaceous framework.[17, 18] This porous texture is generated during the pyrolysis process, where the removal of tar, bound water, and volatile organic matter at elevated temperatures leads to the development of abundant pores and, consequently, a high specific surface area. Compared to the raw corncob, which showed a compact structure with few visible pores, and Bio 400, which exhibited only slight roughness with limited porosity, BioP-Na 400 displayed a highly porous, sponge-like surface with numerous interconnected channels. Such a structure provides favorable pathways for dye molecules to diffuse and adsorb. At higher pyrolysis temperatures, the surface became denser, in agreement with BET results indicating partial pore collapse.

The EDX analysis of raw corncob revealed that the raw corncob was mainly composed of carbon 48.48% and oxygen 42.02%, with a small fraction of phosphorus 0.37%. After pyrolysis at 400°C (Bio 400), the carbon content increased to 71.54% while oxygen decreased to 24.94%, reflecting partial carbonization. In the modified samples, BioP-Na 400 and BioP-Na 500 contained higher carbon levels 77.87% and 76.73%, respectively and introduced sodium 1.03–1.53% together with phosphorus 0.34–0.47%. At 600 °C, BioP-Na 600 reached the highest carbon content

88.86% with a sharp reduction in oxygen 8.86%, while phosphorus rose to 1.69% and sodium decreased to 0.58%. These changes confirm the success of chemical activation, which increased carbonization, reduced oxygen, and incorporated Na and P into the biochar structure.

Taken together, the characterization results demonstrate that BioP-Na 400 possesses the most favorable combination of high surface area, developed mesoporosity, and abundant oxygen-containing functional groups, all of which contribute to efficient adsorption of crystal violet. In contrast, biochars produced at higher pyrolysis temperatures, although richer in carbon content, suffer from pore collapse and reduced surface functionalities, limiting their adsorption performance. These outcomes highlight the importance of optimizing pyrolysis and activation conditions in designing biochar-based adsorbents for dye removal applications.

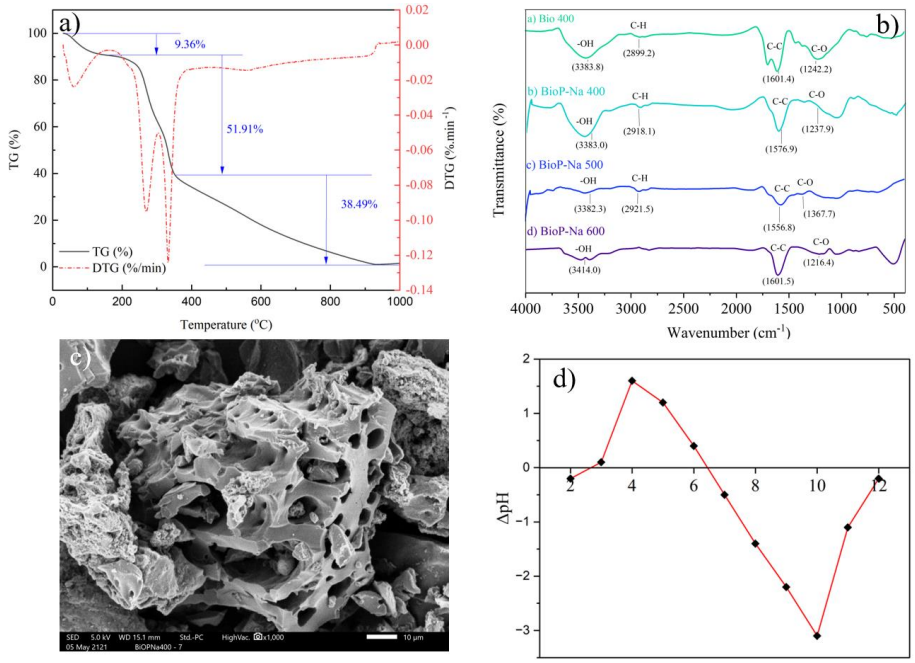

***Figure 1**. Characterization of CC-based materials. Thermal weight loss of CC material (a). FT-IR spectra of biochar at three pyrolysis temperatures (b). SEM micrographs of BioP-Na 400 (c). Point of zero charge (pHpzc) for BioP-Na 400 (d).*[12]

By determining the material's point of zero charge (pH_{pzc}), or the pH at which the surface has no net electrical charge and the cation and anion exchange capacities are balanced, the surface charge of the material was evaluated. It was found in **Figure 1d** that the pH_{pzc} for BioP-Na 400 was determined to be around 6.7. This shows that the surface of the biochar contains a positive charge because of the adsorption of hydrogen ions (H^+) when the pH of the solution is lower than 6.7. On the other hand, the surface becomes negatively charged due to the discharge of hydrogen ions when the pH rises above 6.7.

3.2. Experimental investigation of CV adsorption

3.2.1. Effect of pyrolysis temperature

Pyrolysis temperature refers to the temperature at which pyrolysis occurs, and it is a crucial factor in determining the physicochemical properties of biochar and its adsorption performance. The experimental investigation was conducted at a contact time of 60 min, an initial CV concentration of 30 mg/L, and a biochar dosage of 0.25 g/L. **Figure 2a** presents the effect of pyrolysis temperature on the adsorption performance of different biochars. It can be observed that the removal efficiency increased from 81.5% for Bio 400 to 97.2% for P-Na 400, while the adsorption capacity improved from 99.01 to 116.68 mg/g. When the pyrolysis temperature was further increased to 500°C and 600°C, the adsorption performance insignificantly changed. This small decline may be attributed to the collapse of pores and the reduction of oxygen-containing functional groups at higher temperatures, which are essential for electrostatic interactions and hydrogen bonding with cationic CV molecules. These results indicate that NaOH and H_3PO_4 activation at 400°C provided the most favorable balance between high surface area, developed porosity, and abundant functional groups, leading to superior adsorption of CV. Therefore, BioP-Na 400 was selected for further investigations of the adsorption behavior and mechanism

.

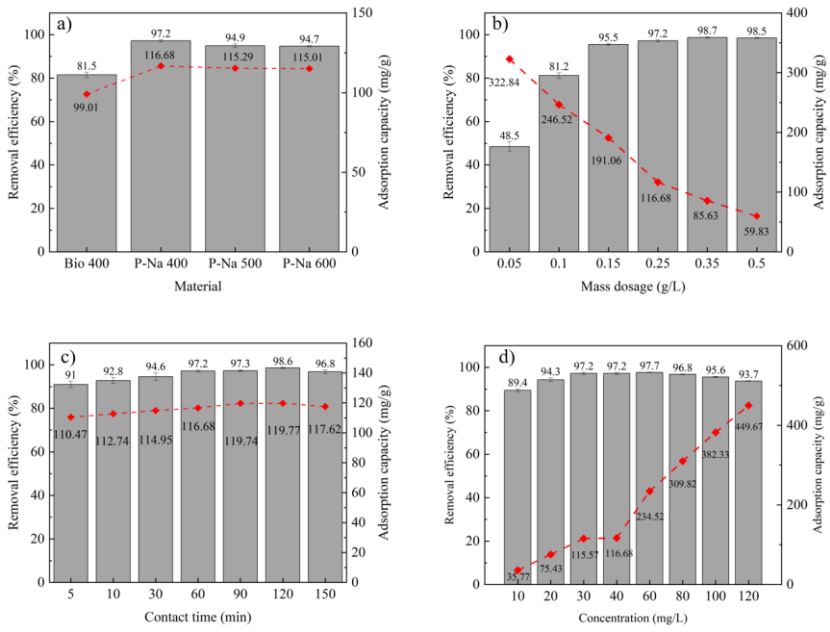

***Figure 2**. The effect of operating parameters on the CV adsorption performance of BioP-Na 400*

3.2.2. Effect of biochar dosage

Adsorbent dosage plays a crucial role in adsorption and significantly influences its performance. The effect of various biochar dosages on CV adsorption was investigated at an initial CV concentration of 30 mg/L, contact

time of 60 min, and biochar dosage ranging from 0.05 to 0.5 g/L. As shown in **Figure 2b**, the adsorption capacity decreased considerably from 322.84 to 59.83 mg/g as the dosage increased. In comparison, the removal efficiency increased sharply from 48.5% at 0.05 g/L to 95.5% at 0.15 g/L, and reached 98.5% at 0.5 g/L, where further increases in dosage no longer improved removal efficiency. The observed trend can be explained by the fact that increasing the amount of biochar provides more available adsorption sites for CV molecules, thereby enhancing the probability of contact between adsorbent and adsorbate. As a result, adsorption equilibrium can be achieved more rapidly with increasing adsorbent dosage. However, at higher dosages, the adsorption capacity per unit mass decreased due to overlapping and aggregation of active sites, which limited the effective utilization of the surface area. Therefore, a dosage of 0.25 g/L was considered optimal for further studies, as it provided high removal efficiency of 97.2% while maintaining a relatively high adsorption capacity of 116.68 mg/g.

3.2.3. Effect of adsorption time

The adsorption time refers to the period required for adsorbate molecules to adhere to the adsorbent surface during the adsorption process. The influence of contact time is therefore crucial for understanding and optimizing adsorption performance. A series of experiments was conducted at an initial CV concentration of 30 mg/L, a biochar dosage of 0.25 g/L, and a contact time ranging from 5 to 150 min. As shown in **Figure 2c**, both removal efficiency and adsorption capacity increased significantly with time at the initial stage. The removal efficiency improved from 91.0% at 5 min to 97.3% at 90 min, while the adsorption capacity increased from 110.47 to 119.74 mg/g in the same period. A slight decrease was then observed with further extension of contact time, reaching 96.8% and 117.62 mg/g at 150 min. The rapid uptake of CV at the beginning of the process can be explained by the abundance of unoccupied active sites on the biochar surface, which allowed dye molecules to be quickly adsorbed. As the available sites became progressively occupied, the adsorption rate slowed down, approaching equilibrium. The slight decrease at prolonged times may be attributed to desorption processes or redistribution of CV molecules between the biochar surface and the bulk solution. According to these findings, an adsorption time of 60 min was considered optimal for further adsorption studies, as it ensured both high removal efficiency (97.2%) and relatively high adsorption capacity (116.68 mg/g).

3.2.4. Effect of CV concentration

The initial adsorbate concentration significantly affects adsorption performance because it governs the driving force for mass transfer between the aqueous phase and the adsorbent surface. In this study, the initial CV concentration ranged from 10 to 120 mg/L, with a biochar dosage of 0.25 g/L and a contact time of 60 min. As presented in **Figure 2d**, the adsorption capacity increased substantially from 35.77 to 449.67 mg/g as the initial concentration increased from 10 to 120 mg/L. In contrast, the removal efficiency first increased slightly from 89.4% at 10 mg/L to a maximum of 97.7% at 60 mg/L, and then

gradually decreased to 93.7% at 120 mg/L. This behavior can be explained by the fact that higher initial concentrations enhance the mass transfer driving force, allowing more CV molecules to diffuse from the solution onto the biochar surface. As a result, the adsorption capacity increased markedly with concentration. However, at elevated concentrations, the limited number of available active sites became saturated, leading to a decline in removal efficiency despite the higher uptake per unit mass.

3.2.5. Adsorption kinetics

Adsorption kinetics were carried out to determine kinetic parameters and the rate at which the adsorption process occurs over time to describe the mechanisms and factors that govern the adsorption process. In this work, the adsorption kinetics of CV onto BioP-Na 400 were determined by fitting the experimental data to various kinetic models involving the pseudo-first-order (PFO), pseudo-second-order (PSO), and Elovich models over a contact time range of 5–150 min, with an initial CV concentration of 30 mg/L and a biochar dosage of 0.25 g/L. These models were described using a nonlinear method, which generally provides more accurate estimations than linearization.[19, 20] The kinetic adsorption data of CV on BioP-Na 400 were analyzed using three kinetic models, and the fitted curves and parameters are presented in **Figure 3a** and **Table 2**, respectively. It was observed that the adsorption capacity (Q_t) of BioP-Na 400 increased sharply with increasing contact time during the first 30 min, followed by a slower increase, and reached equilibrium after approximately 90–120 min with an experimental adsorption capacity of about 119 mg/g. As shown in Table 2, the experimental data were well fitted to the Elovich model with the highest correlation coefficient R^2 = 0.999, indicating that the adsorption occurred on a heterogeneous surface with adsorption energy distributed across different active sites. The PSO model also exhibited a high correlation R^2 = 0.998, with the calculated equilibrium adsorption capacity 118.4 mg/g closely matching the experimental value, suggesting that physical and chemical interactions may contribute significantly to the adsorption process. In contrast, the PFO model gave a slightly lower correlation R^2 = 0.993, indicating that physical adsorption alone could not adequately describe the adsorption mechanism. Additionally, the R^2 value of the PSO was greater than 0.9, which is used for the adsorption process at a low initial adsorbent concentration, at the final stage, and with abundant active sites on the adsorbent surface.[13] Taken together, these results suggest that the CV adsorption process on BioP-Na 400 is a multistep and multimechanistic process with the presence of both physical and chemical interactions.

3.2.6. Adsorption isotherms

Adsorption isotherms describe the relationship between the solute concentration in the bulk solution and the amount of adsorbate retained on the adsorbent surface under equilibrium conditions. Their analysis provides useful information about the adsorption mechanism and the nature of interactions between the adsorbent and adsorbate. In this study, three equilibrium models, namely Langmuir, Freundlich, and Dubinin–

Radushkevich (D–R), were employed to fit the experimental data to better understand the adsorption behavior of CV on BioP-Na 400. The fitted curves and parameters of these models are shown in Figure 3 and Table 3, respectively. It can be seen that the Langmuir model with a higher R^2 value 0.982 provided the best fit for the adsorption process in this study. This result implies that the adsorption of CV onto BioP-Na 400 could be well represented by monolayer adsorption on a relatively homogeneous surface. The maximum adsorption capacity estimated from the Langmuir model was 379.25 mg/g, which is higher than the actual maximum adsorption value observed under the experimental conditions. This difference may be attributed to the limited CV concentration range used in the experiments. In addition, the separation factor (R_L) was lower than 1, confirming that the adsorption of CV was favorable under the studied conditions. The R^2 values of the Freundlich and Dubinin–Radushkevich (D–R) models were also relatively high (0.882 and 0.942, respectively), suggesting that both models could describe the process to some extent. The n value of the Freundlich model was 3.46, which lies in the range of 1–10, indicating that BioP-Na 400 could effectively adsorb CV molecules even at low concentrations, which is advantageous for wastewater treatment applications.[15, 21] Furthermore, the mean adsorption energy obtained from the D–R model was 1.9 kJ/mol, which is much lower than 8 kJ/mol. This finding indicates that the adsorption of CV in this study was mainly physical adsorption.

This conclusion is consistent with the kinetic adsorption results (**Table 2**). The best fit with the Elovich (R^2 = 0.999) and PSO models (R^2 = 0.998) indicated that the process occurred on a heterogeneous surface with contributions from both physical and chemical interactions. Complementary isotherm analysis further showed that the Langmuir model (R^2 = 0.982) most accurately represented the equilibrium data, suggesting monolayer adsorption with a theoretical maximum capacity of 379.25 mg/g, and the separation factor confirmed the favorability of the process, suggesting that the overall process was mainly governed by physical interactions. Overall, these findings confirm that CV adsorption onto BioP-Na 400 is primarily driven by physisorption, supported by heterogeneous surface interactions, making it a promising and efficient adsorbent for practical wastewater treatment application.

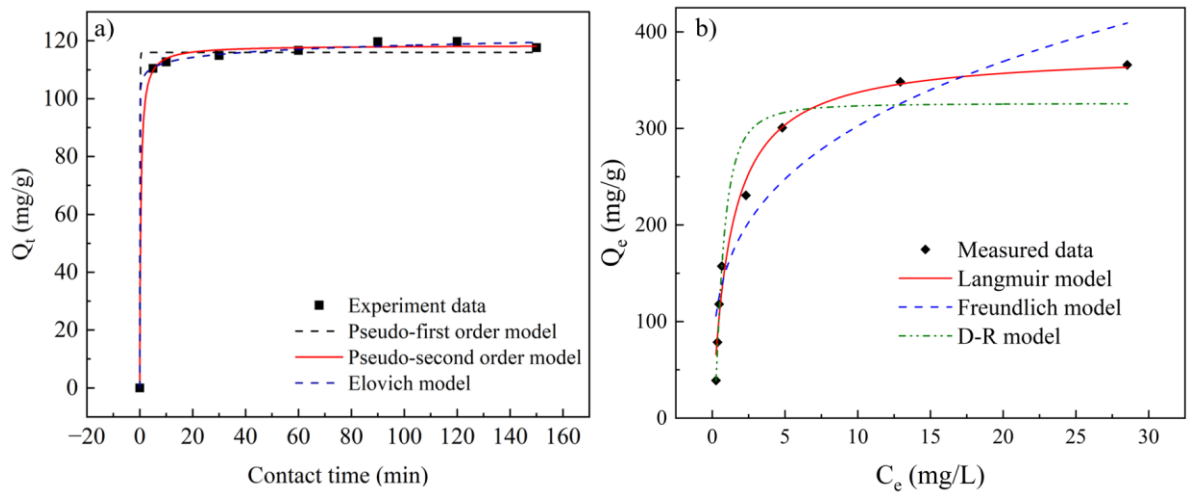

Figure 3. *Adsorption kinetics (a) and adsorption isotherms (b) fitting curves of CV on BioP-Na 400*

Table 2. *Kinetic parameters of CV adsorption on BioP-Na 400*

PFO model			PSO model			Elovich model		
Q_e (mg/g)	K_1	R^2	Q_e (mg/g)	K_2	R^2	A (mg/(g.min))	B (g/mg)	R^2
115.99	25.05	0.993	118.42	2.19	0.998	2.853	0.389	0.999

Table 3. *Isotherm parameters of DBF adsorption on BioP-Na 400*

Langmuir model			**Freundlich model**			**D-R model**		
K_L	Q_m (mg/g)	R^2	K_F	n	R^2	Q_0 (mg/g)	E (kJ/mol)	R^2
0.8	379.25	0.982	155.68	3.46	0.882	325.88	1.9	0.942

4. ADSORPTION MECHANISM OF CV

Based on the adsorption isotherm and kinetic results, important insights into the adsorption mechanism of CV by BioP-Na were obtained. Experimental data analysis showed that the Langmuir isotherm, the Elovich model, and the pseudo-second-order (PSO) kinetic model best fitted the adsorption process, indicating that physical adsorption played a predominant role, mainly occurring on a homogeneous surface with monolayer adsorption of CV. The dominance of physisorption can be attributed to the structural features of the material, including its large specific surface area, high pore volume, and

well-developed pore diameter, which facilitated the diffusion of CV molecules (1.33 nm) into the porous structure.[22] In addition, electrostatic interactions between surface functional groups and CV molecules further enhanced adsorption efficiency. FTIR spectra confirmed the presence of oxygen-containing functional groups such as hydroxyl and carboxyl, which could form hydrogen bonds with the functional groups of CV. Moreover, π–π interactions between the aromatic rings of the biochar structure and CV molecules were also possible. The combination of these mechanisms not only improved the removal performance of CV but also highlighted the potential application of BioP-Na as an effective adsorbent for wastewater treatment containing cationic dyes.[23] The proposed adsorption mechanism is illustrated in **Figure 4**.

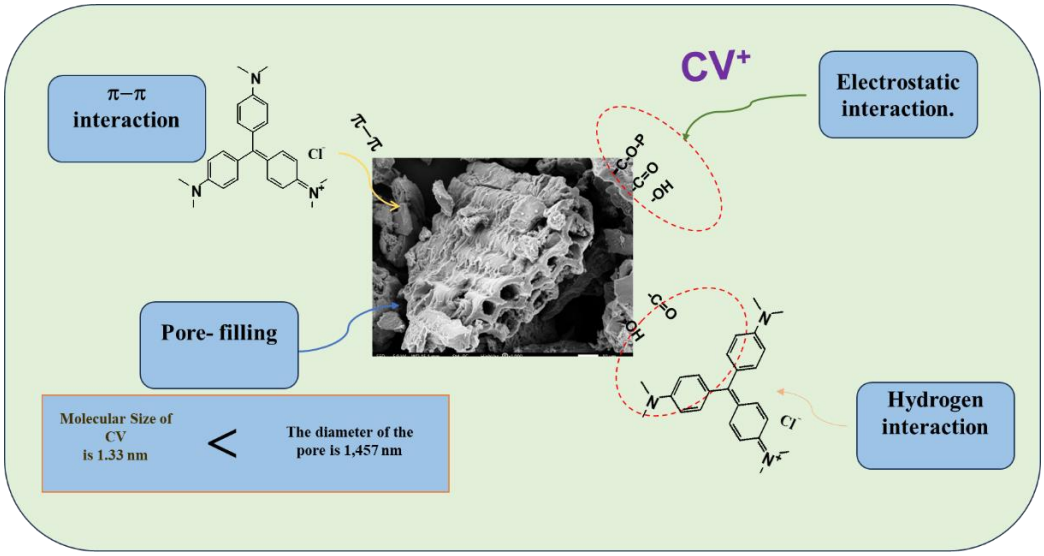

Figure 4. *Adsorption mechanism of CV*

5. CONCLUSION

This study confirmed that modified corn cob biochar, particularly BioP-Na 400, is an efficient adsorbent for crystal violet (CV) removal from aqueous solutions. The material exhibited a high specific surface area, well-developed mesoporosity, and abundant functional groups, which collectively contributed to its superior adsorption performance. Under optimal conditions, BioP-Na 400 achieved a removal efficiency of 97.2% and a maximum adsorption capacity of 116.68 mg/g at an initial CV concentration of 30 mg/L within 60 minutes. Kinetic analyses indicated that the adsorption process followed the Elovich (R^2 = 0.999) and pseudo-second-order (R^2 = 0.998) models, suggesting heterogeneous surface interactions involving both physical and chemical adsorption. Isotherm studies showed that the Langmuir model (R^2 = 0.982) best fitted the equilibrium data, confirming monolayer adsorption with a theoretical maximum capacity of 379.25 mg/g. Complementary analysis of the Dubinin–Radushkevich model revealed that the overall process was mainly governed by physical interactions. Overall, these results demonstrate that corn cob-derived

biochar, especially BioP-Na 400, is a promising low-cost and eco-friendly adsorbent. The findings highlight the potential of valorizing agricultural residues into functional materials for sustainable wastewater treatment and environmental protection.

REFERENCES

1. W. Zhang, H. Li, X. Kan, L. Dong, H. Yan, Z. Jiang, H. Yang, A. Li and R. Cheng., Adsorption of anionic dyes from aqueous solutions using chemically modified straw, *Bioresource Technology,* **2012**, *117*, 40-47
2. E. Q. Adams, L. Rosenstein, THE COLOR AND IONIZATION OF CRYSTAL-VIOLET, *Journal of the American Chemical Society,* **1914**, *36*(7), 1452-1473.
3. S. Mona, A. Kaushik, and C. Kaushik, Waste biomass of Nostoc linckia as adsorbent of crystal violet dye: optimization based on statistical model, *International Biodeterioration & Biodegradation,* **2011**, *65*(3), 513-521.
4. M. P. Shah, K. A. Patel, and S. S. Nair, Microbiological removal of crystal violet dye by Bacillus subtilis ETL-2211, *OA Biotechnol,* **2013**, *2*(9).
5. S. Mani, R. N. Bharagava, Exposure to crystal violet, its toxic, genotoxic and carcinogenic effects on environment and its degradation and detoxification for environmental safety, *Reviews of Environmental Contamination and Toxicology*, **2016**, *237,*71-104.
6. G. B. Michaels and D. L. Lewis, Sorption and toxicity of azo and triphenylmethane dyes to aquatic microbial populations, *Environmental toxicology and chemistry*, **1985**, *4*(1), 45-50.
7. S. Moon, J. Ryu, J. Hwang, and C.-G. Lee, Efficient removal of dyes from aqueous solutions using short-length bimodal mesoporous carbon adsorbents, *Chemosphere*, **2023**, *313*, 137448.
8. M. V. Trịnh, T. V. Cường, V. D. Quỳnh, and N. T. H. Thu, Nghiên cứu sản xuất than sinh học từ rơm rạ và trấu để phục vụ nâng cao độ phì đất, năng suất cây trồng và giảm phát thải khí nhà kính, *Tạp chí Khoa học và Công nghệ Nông nghiệp Việt Nam*, **2011**,66-69.
9. T. M. Vũ, V. T. Trịnh, Nghiên cứu khả năng xử lý amoni trong môi trường nước của than sinh học từ lõi ngô biến tính bằng H_3PO_4 và NaOH, *VNU Journal of Science: Earth and Environmental Sciences*, **2016**, *32(1S)*.
10. V. N. X. Que, T. T. Khoi, N. T. Thuy, T. T. M. Dung, D. T. T. Binh, and N. N. Huy, Factors determining the removal efficiency of Procion MX in waters using titanate nanotubes catalyzed by UV irradiation, *Journal of Nanotechnology*, **2021**, 2021(1), 8870453.
11. S. Kumar, Y. S. Negi, and J. S. Upadhyaya, Studies on characterization of corn cob based nanoparticles, *Adv. Mater. Lett*, **2010**, *1(3)*, 246-253.
12. N. T. Q. T. Châu Thiên Ân, Cải thiện khả năng xử lý Methyl Violet bằng than sinh học biến tính từ lõi ngô, Graduation thesis, Faculty of Chemical Engineering, Can Tho University, **2024**.
13. J. Wang and X. Guo, Adsorption kinetic models: Physical meanings, applications, and solving methods, *Journal of Hazardous materials*, **2020**, *390*, 122156.
14. C. Tejada-Tovar, Á. Villabona-Ortíz, and Á. D. Gonzalez-Delgado, Removal of nitrate ions using thermally and chemically modified bioadsorbents, *Applied Sciences*, **2021**, *11*(18), 8455.
15. T. Wang, D. Zhang, K. Fang, W. Zhu, Q. Peng, and Z. Xie, Enhanced nitrate removal by physical activation and Mg/Al layered double hydroxide modified biochar derived from wood waste: Adsorption characteristics and mechanisms, *Journal of Environmental Chemical Engineering*, **2021**, *9*(4), 105184.
16. T. Wang, J. Zheng, H. Liu, Q. Peng, H. Zhou, and X. Zhang, Adsorption characteristics and mechanisms of Pb^{2+} and Cd^{2+} by a new agricultural waste–Caragana korshinskii biomass derived biochar, *Environmental Science and Pollution Research*, **2021**, *28*(11), 13800-13818.
17. W. A. W. A. K., Ghani, A. Mohd, G. da Silva, R.T, Bachmann, Y.H, Taufip-Yap, *U. Rashid and A.A.H, Al-Mutaseb.*, Biochar production from waste rubber-wood-sawdust and its potential use in C sequestration: chemical and physical characterization, *Industrial Crops and Products*, **2013**, *44*, 18-24.
18. L. D. Hafshejani, A. Hooshmand, A. A. Naseri, A. S. Mohammadi, F. Abbasi, and A. Bhatnagar, Removal of nitrate from aqueous solution by modified sugarcane bagasse biochar, *Ecological Engineering*, **2016**, *95*, 101-111.

19. M. I. El-Khaiary, G. F. Malash, Y.-S. Ho, On the use of linearized pseudo-second-order kinetic equations for modeling adsorption systems, *Desalination*, **2010***, 257(1-3)*, 93-101.

20. K. V. Kumar, S. Sivanesan, Pseudo second order kinetics and pseudo isotherms for malachite green onto activated carbon: comparison of linear and non-linear regression methods, *Journal of Hazardous Materials*, **2006***, 136(3)*, 721-726.

[21] M. I. Inyang, B. Gao, Y. Yao, Y. Xue, A. Zimmerman, A. Mosa, P. Pullammanappallil, Y.S. Ok and X. Cao., A review of biochar as a low-cost adsorbent for aqueous heavy metal removal, *Critical reviews in environmental science and technology*, **2016***, 46*(4), 406-433.

22. S. Chowdhury, S. Chakraborty, and P. Das, Adsorption of crystal violet from aqueous solution by citric acid modified rice straw: equilibrium, kinetics, and thermodynamics, *Separation Science and Technology*, **2013***, 48*(9), 1339-1348.

23. B. T. Gemici, Crystal violet adsorption onto modified biosorbent prepared from agricultural waste: kinetics, isotherm and thermodynamic studies, *Chemical Engineering Communications*, **2024***, 211*(4), 582-591.